THE JOURNAL OF PHYSICAL CHEMISTRY C

Article

pubs.acs.org/JPCC

X-ray Spectroscopic Characterization of Immobilized Rhenium Species in Hydrated Rhenium−Palladium Bimetallic Catalysts Used for Perchlorate Water Treatment

Jong Kwon Choe,[†] Maxim I. Boyanov,[‡] Jinyong Liu,[†] Kenneth M. Kemner,[‡] Charles J. Werth,[†] and Timothy J. Strathmann*,[†]

[†]Department of Civil and Environmental Engineering, University of Illinois at Urbana−Champaign, Urbana, Illinois 61801 United States

[‡]Biosciences Division, Argonne National Laboratory, Argonne, Illinois 60439 United States

Supporting Information

ABSTRACT: Carbon-supported rhenium−palladium catalysts (Re−Pd/C) effectively transform aqueous perchlorate, a widespread drinking water pollutant, via chemical reduction using hydrogen as an electron donor at ambient temperature and pressure. Previous work demonstrated that catalyst activity and stability are heavily dependent on solution composition and Re content in the catalyst. This study relates these parameters to changes in the speciation and molecular structure of Re immobilized on the catalyst. Using X-ray spectroscopy techniques, we show that Re is immobilized as Re^{VII} under oxic solution conditions, but transforms to a mixture of reduced, O-coordinated Re species under reducing solution conditions induced by H_2 sparging. Under oxic solution conditions, extended X-ray absorption fine structure (EXAFS) analysis showed that the immobilized Re^{VII} species is indistinguishable from the dissolved tetrahedral perrhenate (ReO_4^-) anion, suggesting outer-sphere adsorption to the catalyst surface. Under reducing solution conditions, two Re species were identified. At low Re loading (≤1 wt %), monomeric Re^{I} species form in direct contact with Pd nanoclusters. With increased Re loading, speciation gradually shifts to oxidic Re^{V} clusters. The identified Re structures support a revised mechanism for catalytic reduction of ClO_4^- involving oxygen atom transfer reactions between odd-valence oxorhenium species and the oxyanion (Re oxidation steps) and atomic hydrogen species (Re reduction steps) formed by Pd-catalyzed dissociation of H_2.

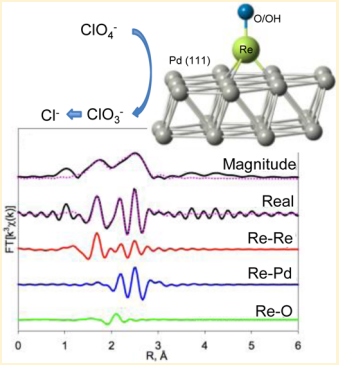

INTRODUCTION

Rhenium (Re) shows great promise in a wide range of catalytic applications due to its strong oxophilic and electrophilic characteristics compared to other transition metals,[1] and supported Re catalysts are widely used in industry for a variety of purposes. Oxides of Re (e.g., Re_2O_7) immobilized on alumina supports are used as catalysts for olefin metathesis in the specialty chemicals and polymer industry.[2] Carbon-supported Re catalysts can also be used for hydrodesulfurization processes in the refining of diesel fuels.[3,4] In addition, bimetallic catalysts incorporating Re (e.g., together with Pt) are applied in the petrochemical industry for naptha reforming and show promise for aqueous phase reforming of biomass-derived oxygenates[5−7] and hydrothermal conversion of lipids to hydrocarbon fuels.[8]

Recent work has shown that adding Re to carbon-supported palladium (Pd) hydrogenation catalysts enables reduction of perchlorate (ClO_4^-) and related aqueous oxyanion contaminants that are harmful to human health in drinking water.[9−12] Chemical reduction of ClO_4^- is especially challenging due to a high activation barrier for electron transfer,[13] and reaction with most water treatment reductant materials is slow or undetectable at ambient temperatures and pressures.[14] Re−Pd/C reduces aqueous ClO_4^- to innocuous Cl^- using H_2 as an electron donor at rates much higher than those reported for other reactive materials.[9−11] The currently proposed catalytic mechanism (Figure 1) involves initial oxygen atom transfer (OAT) from ClO_4^- to immobilized Re^{V}, yielding ClO_3^- (chlorate) and Re^{VII}. Re^{VII} is then re-reduced to Re^{V} by Pd-adsorbed atomic hydrogen (Pd−H_{ads}) formed via dissociation of exogenous H_2.[9,12] Sequential OAT reaction cycles and direct reaction with Pd−H_{ads} then rapidly reduce ClO_3^- to Cl^-.

Previous work in our group demonstrated that Re−Pd/C catalyst activity and stability are heavily dependent on the Re content (wt %) of the catalyst and on the redox chemistry of the overlying aqueous solution (i.e., air-sparged oxic solution conditions versus H_2-sparged reducing conditions).[11] X-ray photoelectron spectroscopy (XPS) analysis showed that these variables affect the oxidation state of the immobilized Re, resulting in species ranging between +7 and +1 in formal oxidation state.[11] Under reducing conditions, two Re species were identified, one tentatively assigned to Re^{V} or Re^{IV} and one

Received: January 20, 2014
Revised: April 24, 2014
Published: May 12, 2014

 © 2014 American Chemical Society

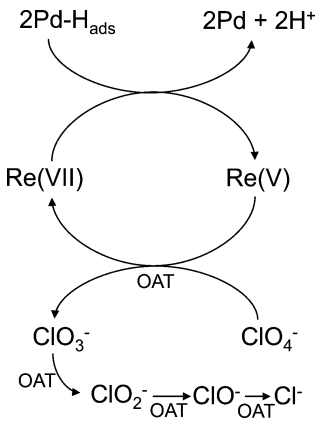

Figure 1. Previously proposed catalytic oxygen atom transfer (OAT) scheme for ClO_4^- reduction to Cl^-.[7] Each OAT cycle involves Re cycling between +5 and +7 oxidation states.

assigned to Re^I,[11] suggesting the need for modification of the previously proposed mechanism for catalytic reduction of ClO_4^-. However, more detailed characterization of Re speciation is necessary to further elucidate the reaction mechanisms and to enable improvements in catalyst performance.

Synchrotron X-ray adsorption spectroscopy (XAS) in the hard X-ray region (5−30 keV) is ideally suited to characterize metal catalysts used for water treatment applications. X-ray absorption near edge structure (XANES) and extended X-ray adsorption fine structure (EXAFS) spectra can provide information on the valence state and local coordination environment of Re in wet catalyst samples, without the need for long-range structural order or extensive sample preparation protocols (e.g., vacuum drying) that may lead to artifacts.[15] Previous studies have used XAS to characterize supported Re catalysts under various conditions. Hardcastle et al.[16] used XANES to identify a Re oxide structure resembling tetrahedral perrhenate (ReO_4^-) when the metal (0.1−12 wt %) was immobilized on alumina (Al_2O_3) support and calcined at 500 °C. Bare et al.[17] used EXAFS to characterize Re/Al_2O_3 (0.7 wt %) exposed to oxidizing (O_2/He, 500 °C) and reducing (H_2, 500 °C, 700 °C) gaseous environments. Under oxidizing conditions, analysis showed Re present as trioxo(oxoaluminate) Re^{VII} species bound to the alumina surface, whereas under reducing conditions the metal was shown to form a mixture of unreduced trioxoaluminate Re^{VII} species, metallic Re nanoclusters, and isolated Re atoms strongly bound to the alumina surface. Supported bimetallic catalysts incorporating Re have also been studied by XAS. Fung et al.[18] investigated $Re_2Pt(CO)_{12}$ supported on alumina (0.32 wt % Pt and 0.59 wt % Re) after treatment with H_2 at 400 °C. Re L_{III} and Pt L_{III} edge EXAFS spectra showed oxygen-coordinated Re atoms on the alumina support and identified Re−Pt and Re−Re coordination. Daniel et al.[19] investigated Pt−Re/C catalysts with higher metal loading (5.7 wt % Pt and 4.6 wt % Re) using EXAFS analysis and observed that Re was partially reduced by H_2 at 200 °C when Pt was present. The study concluded that Re exists as a mixture of atomically dispersed oxidized Re on the Norit activated carbon surface and reduced Re associated with bimetallic nanoparticles with diameter ≤1 nm.

Most prior studies on Re catalysts only provided spectroscopic information on the catalysts in "dried form" under various flowing gas conditions (e.g., H_2, O_2, air) and at elevated temperatures.[6,19−21] A limited examination of the effect of water vapor in the flowing gas mixture was presented in Bare et al.,[17] showing significant changes in Re speciation relative to catalysts exposed to dry gases. Because Re−Pd/C catalysts used for ClO_4^- treatment are prepared and applied in aqueous solution at ambient temperatures, XAS analysis of wet catalyst samples prepared with minimal sample alteration is desirable to accurately identify the structures of Re species present in the active catalyst under in situ reaction conditions.

This contribution describes Re L_{III} edge XAS analysis of the speciation of Re immobilized on carbon-supported Re−Pd bimetal catalysts following exposure to oxic or reducing aqueous solution conditions. The influence of Re content (wt %) was explored to provide insights into previously reported reactivity trends.[9] Results obtained from bulk XAS characterization of Re in wet catalyst samples were compared to those from surface-sensitive XPS characterization of dried samples. Structural information obtained from analysis with complementary X-ray spectroscopic techniques provides further mechanistic insights into the catalyst's reactivity with oxyanion contaminants and stability during water treatment applications.

■ EXPERIMENTAL SECTION

Chemical Reagents and XAS Standards. Re metal, rhenium dioxide (ReO_2), rhenium trioxide (ReO_3), and ammonium perrhenate (NH_4ReO_4) were purchased from Sigma-Aldrich. A Re^V reference standard, Re(O)(*hoz*)$_2$Cl (*hoz* = 2-(2′-hydroxyphenyl)-2-oxazoline), was synthesized from potassium perrhenate ($KReO_4$) following reported methods.[22−24] A Pd catalyst (nominally 5 wt % Pd) on activated carbon powder support (Pd/C, wet Degussa type E101) was also purchased from Sigma-Aldrich. Previous analysis indicated a Pd content of 4.65 wt %, 28.2% Pd dispersion, and BET specific surface area of 892 $m^2\ g^{-1}$.[11,25] Reagent-grade HCl and NaOH were obtained from Fisher Scientific. Purified H_2 (99.999%) and air (99.9%) were obtained from Matheson Tri-Gas (Joliet, IL). Deionized water (electrical resistivity > 17.8 MΩ cm; Barnstead Nanopure system) was used in all experiments.

Sample Preparation. Re−Pd/C catalysts with different Re loadings were prepared according methods described previously.[11] Briefly, Pd/C particles <37 μm in diameter were collected by wet sieving. The powders were then dried in air for 1 h at 110 °C and heated to 250 °C for 1 h under flowing H_2 before cooling to room temperature. For Re immobilization, 0.5 g Pd/C was added to 250 mL water in a flask under continuous stirring at room temperature. For exposure to reducing solution conditions (i.e., representative of conditions used to catalyze ClO_4^- reduction), the catalyst suspension was continuously sparged with H_2 gas at a rate of 200 mL/min, and HCl was added to adjust pH to 2.7. After the desired quantity of NH_4ReO_4 was introduced to yield 0.5−12 wt % Re, the reactor was mixed for 5 h to immobilize the added Re. The resulting catalyst suspension was then transferred into an anaerobic glovebox chamber (97% N_2, 3% H_2) and a wet paste of catalyst particles (∼53 wt % H_2O) was collected by vacuum filtration. For exposure to oxic solution conditions, the aqueous catalyst suspension was adjusted to pH 2.7 (which makes the Pd/C surface have a net positive charge when exposed to the oxic water) and mixed under air atmosphere for 5 h before collecting a wet paste of catalyst particles by vacuum filtration conducted outside the glovebox. Our previous study[11] showed nearly complete adsorption of Re to Pd/C in oxic aqueous

suspensions at ReO_4^- concentrations corresponding to up to ~6 wt %Re and nearly complete immobilization of up to ~15 wt % Re on the catalyst when suspended in water under reducing solution conditions.

For XAS analysis, the wet catalyst pastes were mounted in slotted Plexiglas sample holders (1″ × 1/8″ × 1/8″ well size) and sealed with Kapton film to avoid exposure to air during sample transport, manipulation and analysis. All sample and standard manipulations were carried out under anoxic conditions. Reference standards were mounted in powder form uniformly deposited on the adhesive side of Kapton tape, which was then folded and sealed. Special care was taken to prevent catalyst sample exposure to air. From inside the anaerobic glovebox chamber, sealed catalyst samples and reference standards were loaded into a glass flask also containing Pd catalyst pellets to scavenge any trace O_2 entering the flask and a moist sponge was added to prevent evaporation of the sealed wet paste samples. The flask was then sealed with a thick rubber stopper and Kapton tape and transported from UIUC (Urbana, IL) to Argonne National Lab (Argonne, IL), where it was immediately transferred into a similar anaerobic glovebox chamber at Argonne until analyzed. XAS data collection occurred within 2 days of sample preparation.

For XPS analysis of catalysts prepared under reducing solution conditions, the vacuum-collected catalyst pastes were dried at 110 °C in a sand bath inside the glovebox and analyzed in dried powder form. While still inside the glovebox, the dried catalyst samples were loaded onto copper conductive tape placed on a steel sample holder. The sampler holder was then placed inside a special anoxic sample chamber designed for air-sensitive samples, sealed, and transported from the glovebox to the instrument. The sample holder was immediately loaded into the instrument and placed under high vacuum ($<10^{-6}$ Torr) to prevent air exposure. Previous work showed that special care was needed to eliminate artifacts from air exposure.[11] For catalysts prepared under oxic solution conditions, catalyst pastes were dried in air at 110 °C in a laboratory oven prior to loading onto the copper tape on the sample holder and transporting to the instrument for analysis.

X-ray Absorption Spectroscopy. X-ray absorption spectra were collected at the MRCAT/EnviroCAT bending magnet beamline (Sector 10-BM) at the Advanced Photon Source (APS) at Argonne National Laboratory.[26] The beamline utilizes a Si(111) double crystal, water-cooled monochromator; detuning of the second crystal to 50% of the maximum intensity was used for higher harmonics rejection. The beam size was set to approximately 3 mm wide and 0.5 mm high. Samples were loaded in a N_2-flushed chamber with Kapton windows to prevent oxygen exposure during data acquisition. Re L_{III} edge spectra were measured in transmission mode over the range of 10335−11500 eV. For catalyst samples and reference standards, 3−8 spectra were collected and averaged. To minimize radiation exposure and to monitor for beam-induced changes in the samples, scans were collected from three fresh locations on each sample. Energy calibration was continuously monitored during data acquisition by simultaneous collection of spectra from a metallic Re sample using X-rays transmitted through the sample of interest.

ATOMS,[27] ARTEMIS,[28] ATHENA,[28] IFEFFIT,[29] and FEFF8[30] programs were used for analysis of the XAS data. Raw spectra were processed using ATHENA for spectral averaging, edge-step normalization, and background removal. The edge positions of the Re reference standards and the catalyst samples were measured at the inflection points (maximum of the XANES first derivative). EXAFS spectral analysis and fitting were performed using ARTEMIS. The k^3-weighed $\chi(k)$ spectra were extracted from the raw data in the k-range of 3.0 to 13.0 $Å^{-1}$. Fourier transforms (FT) of the k^3-weighed $\chi(k)$ spectra were then obtained for the same k range using a 1.0 $Å^{-1}$ wide Hanning window sill.

For EXAFS data fitting, the known crystallographic structures of ReO_2[31] and NH_4ReO_4[32] were used to generate FEFF input files from ATOMS. FEFF 8.0 was then used to calculate backscattering phase and amplitude functions of single-scattering Re−O and Re−Re paths. A Re−Pd single-scattering path was generated by substituting backscattering Re with Pd in the FEFF input file created from the ReO_2 crystal structure (No reported crystal structure containing both Re and Pd was identified by the authors). Measured data were fit by varying the coordination number (CN), interatomic distance (R), energy shift (ΔE^0), and Debye−Waller factor (σ^2) for each scattering path, employing various constraints to reduce the number of variables. The passive electron amplitude reduction factor (S_0^2) was determined from analysis of two Re reference compounds, ReO_2 and NH_4ReO_4, by fitting the EXAFS data with fixed coordination numbers based on the reported crystal structures. The S_0^2 values were 0.86 and 0.88 for ReO_2 and NH_4ReO_4, respectively, and the average value of 0.87 was used for model fits of the catalyst samples. The spectral data and the model fits of the two reference compounds are provided in Supporting Information (SI). The Fourier transform (FT) of the data were fit in the range $R + \Delta = 1.4$−3.0 Å using a combination of Re−O, Re−Re, and Re−Pd scattering paths.

Previous XPS analysis in our laboratory showed the presence of two Re species on the surfaces of catalysts obtained under reducing solution conditions. XANES and EXAFS analysis in the present study (discussed below) shows that one Re species is predominant in the 12 wt % Re catalyst (one of two compositional endmember samples), whereas two Re species are significant in the 0.5 wt % Re catalyst (the other endmember). For analysis of the 12 wt % Re catalyst, the EXAFS data were fit using a combination of Re−O and Re−Re scattering paths and interpreted as Re cluster species. Additional species in the 12 wt % Re catalyst were quantified at <10% of total Re (see below), which is within the uncertainty of the EXAFS analysis. The potential presence of such species therefore does not affect the structural conclusions in a significant manner. To account for the partial contribution of the Re cluster species in the 0.5 wt % Re catalyst data, the structural parameters for the Re−O and Re−Re scattering paths were fixed to those determined from fits of the 12 wt % Re catalyst and the coordination numbers were multiplied by a fractional fitting parameter x ($0 < x < 1$). The remaining part of the spectrum was attributed to other Re species, whose spectral contribution was fit using combinations of unconstrained Re−O, Re−Re, and Re−Pd single scattering paths. The obtained coordination numbers for shells corresponding to this second immobilized Re species were divided by $(1 - x)$ before interpreting the structure. The structures of the Re species were visualized using CrystalMaker (CrystalMaker Software Ltd.).

To quantify the proportions of these two different Re species in samples of intermediate Re loading, the k^3-weighted $\chi(k)$ data from all catalysts were fit with linear combinations of spectra extracted for the two Re species using the following equation,

$$\chi(k) = y \times \chi_1(k) + (1 - y) \times \chi_2(k) \text{ for } 0 < y < 1$$

where $\chi_1(k) = k^3\chi(k)$ derived for Re species 1 (referred to as cluster species) and $\chi_2(k) = k^3\chi(k)$ derived for Re species 2 (later referred to as monomeric species) in the shell-by-shell fits of the 0.5 and 12 wt % endmembers.

X-ray Photoelectron Spectroscopy. To complement the XAS data, surface chemical compositions and oxidation states of Re were also analyzed by XPS using a Physical Electronics PHI 5400 X-ray photoelectron spectrometer. A monochromatized Mg Kα source was used. Re 4f spectra were collected and energy-normalized to the C 1s peak (binding energy of 284.5 eV). The source of the C peak was adventitious carbon for the Re reference compounds and the activated carbon support for catalyst samples. High resolution (i.e., 0.1 eV resolution with pass energy of 35.75 eV) Re spectra were obtained by collecting 100 scans per sample. Individual Re species exhibit Re $4f_{7/2}$ and Re $4f_{5/2}$ doublet peaks that are separated by 2.43 eV and have relative peak areas with a fixed ratio of 4:3.[33] The chemical state of Re species is typically characterized by the binding energy (BE) of the Re $4f_{7/2}$ peak position. Spectra of the catalyst samples were normalized and fit with a convoluted Gaussian and Lorentzian function (using CasaXPS ver.2.3) after constraining the separation distance and peak area ratio of contributing doublet peaks. When spectra indicated the presence of two Re species, the relative proportions and characteristic binding energies of the contributing species were determined by linear combination fitting of two doublet peak sets (each doublet peaks corresponding to a characteristic Re species) using the same constraints as described above.

■ RESULTS

XANES and XPS Analysis. Rhenium L_{III}-edge XANES spectra of the catalyst samples and reference standards of varying oxidation state (metallic Re, $Re^{IV}O_2$, $Re^{V}(O)(hoz)_2Cl$, $Re^{VI}O_3$, and $NH_4Re^{VII}O_4$) are shown in Figure 2A (overlays of the same spectra are provided in Figures S1−S3 in Supporting Information). The absorption edge position and the whiteline (resonance) intensity is sensitive to the formal oxidation state and coordination geometry of Re.[34] The reference spectra show that the edge position shifts to higher energies as the formal oxidation state increases from metallic to oxidized states. Following previous studies,[5,17] an empirical correlation between the edge position and Re oxidation state of reference standards was developed (Figure 2B, square symbols) that can be applied to estimate the average Re oxidation state in the unknown catalyst samples.

The XANES spectrum of the 5 wt % Re5 wt % Pd/C catalyst sample under oxidizing solution conditions (i.e., air-saturated water) shows an absorption edge position that is identical to that of the NH_4ReO_4 reference standard (Figures 2A and S2). This indicates that Re immobilized at the surface of the catalyst exposed to oxic solution conditions has an average oxidation state of +7, in agreement with prior XPS characterization of the same catalyst.[11] The transmission XANES whiteline intensity and the post edge features of the catalyst sample are more similar to those of the NH_4ReO_4 reference standard after dissolution in water than in the solid form (Figure S2). This suggests that in oxic water, the prevailing Re species associated with the Pd/C catalyst surface are solvated ReO_4^- ions adsorbing via outer-sphere complexation mechanisms rather than NH_4ReO_4 surface precipitates. EXAFS analysis (next section) supports the same conclusion.

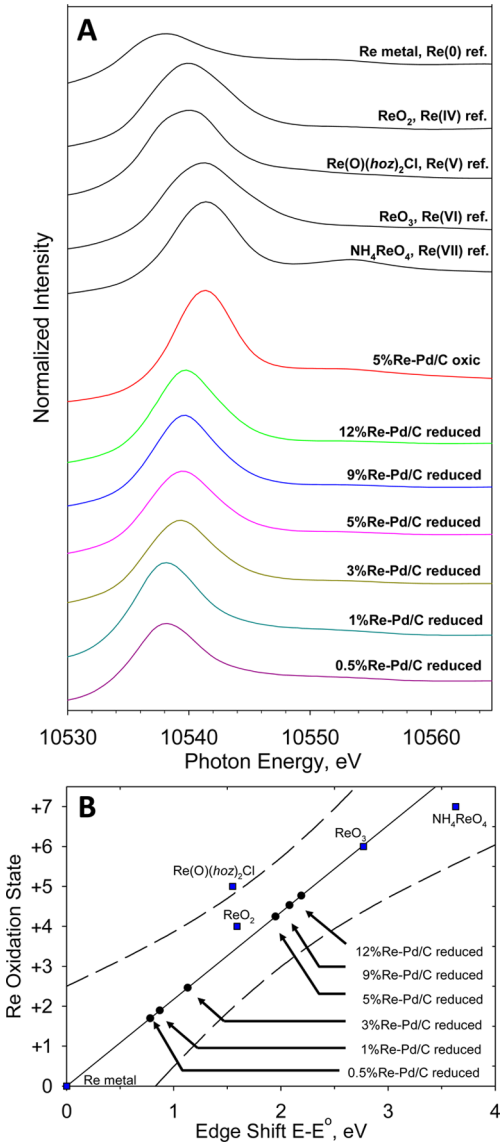

Figure 2. Re L_{III} edge XANES spectral analysis of Re−Pd/C samples. (A) Comparison of Re reference standards and 0.5−12 wt % Re−5 wt % Pd/C samples collected from solution under oxic versus reducing solution conditions, and (B) correlation of the oxidation states vs Re L_{III} edge positions of Re reference standards (squares) and application of the correlation to estimate the average oxidation state of Re present in catalyst samples (circles) with different Re content prepared under reducing solution conditions. $E - E^0$ represents the difference between the edge position of target compound and the edge position of Re metal.

In comparison to the XANES spectrum of the catalyst exposed to oxic solution conditions, the edge positions are shifted to lower energies for catalysts exposed to reducing solution conditions (by continuous H_2 sparging of the overlying solution), and the edge positions vary with Re content (Figures 2A and S1). The edge position for the catalyst sample with the highest Re content (12 wt %) falls between the position observed for ReO_3 (+6 reference standard) and the positions observed for ReO_2 (+4 reference standard) or $Re(O)(hoz)_2Cl$ (+5 reference standard). Application of the empirical correlation in Figure 2B yields an average apparent oxidation state of +4.8 ± 1.4. With decreasing Re content, the edge position gradually shifts to lower energies. For the catalyst

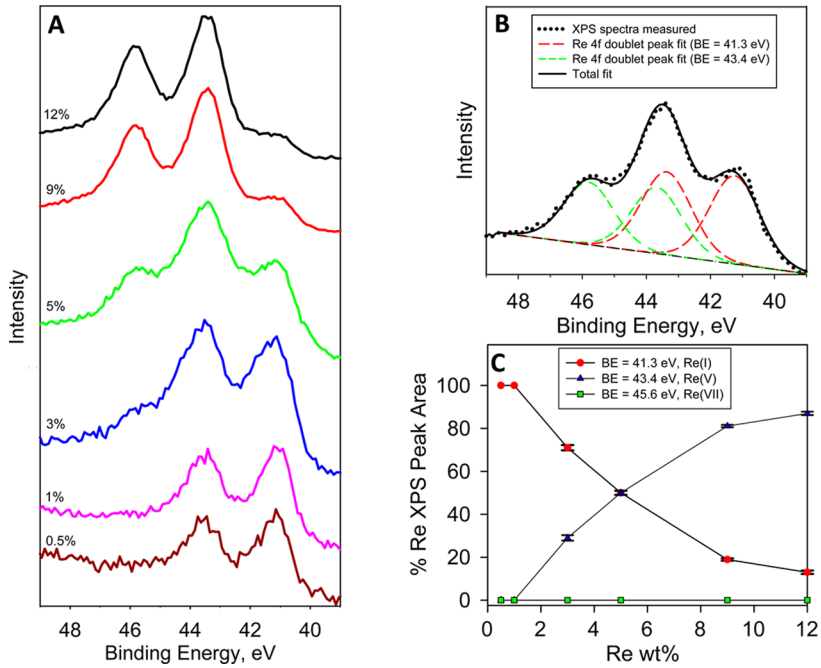

Figure 3. (A) Re 4f XPS spectra of 0.5−12 wt % Re−5 wt % Pd/C catalysts collected from water under reducing conditions (continuous $H_{2(g)}$ sparging), (B) measured spectrum of 5 wt % Re−5 wt % Pd/C catalyst with spectral fit, and (C) effect of Re content on the proportions of spectral fits contributed by doublet peaks with binding energies characteristic of different Re oxidation states. Data for 3−12 wt % were obtained from a previous study.[8] Error bars indicate 95% confidence levels.

samples with lowest Re content (0.5−3 wt %), the edge positions fall between metallic Re (+0 reference standard) and the +4/+5 reference standards. Even though the edge positions of the 0.5 and 1 wt % are close to that of metallic Re, the whiteline intensities for the catalyst samples are significantly larger than that observed for the metallic Re reference standard (Figure S1). The peak intensity for the Re metal standard here (∼2.1, Figure S1) is similar to previous reports,[17,19,20] indicating that the lower intensity in the standard is not an artifact resulting from sample thickness. Thus, the consistently larger whiteline amplitudes observed in the catalyst samples relative to the metallic Re indicate that the immobilized Re species have ionic character. This conclusion is further supported by the lack of postedge resonance feature of bulk metallic Re observed at ∼10554 eV (see arrow in Figure S1) and by the EXAFS data (next section). Application of the empirical correlation in Figure 2B yields an average oxidation state of +1.6 ± 1.7 for the catalyst with 0.5 wt % Re. For catalyst samples with 1−9 wt % Re, the average oxidation state increases with Re content and falls between the values determined for the compositional endmembers. The gradual increase in apparent oxidation state is presumed to result from changes in the distribution of Re species in the samples (e.g., changing proportions of Re^V and Re^I species).

Surface-sensitive XPS data (Figure 3) for catalysts exposed to reducing solution conditions indicate similar patterns in Re valence state as the bulk XANES data. Individual Re 4f XPS spectra (Figure 3A) show characteristic doublet peaks for each Re species, resulting from spin−orbit coupling effects. For catalyst samples with low Re content (e.g., 0.5−1 wt %), spectra could be fit with a single constrained doublet (double peak separation and peak area ratio constrained as described in the Experimental Section) with Re $4f_{7/2}$ peak position at binding energy (BE) of 41.3 eV. At higher Re contents (e.g., 5 wt %), successful spectral fits require two contributing doublets (Figure 3B), with Re $4f_{7/2}$ BE = 41.3 and 43.4 eV. These Re $4f_{7/2}$ BE values correspond closest to those obtained for Re reference standards with +1 and +5 oxidation states, respectively. Figure 3C shows that the spectra of catalyst samples with 0.5−12 wt % Re can be fit by a combination of these two Re species in different proportions. The distribution of species shifts to more oxidized species (BE = 43.4 eV) as Re content increases, reaching a maximum value of ∼85% Re^V when total Re content is increased to 12 wt %. The same general pattern is observed with XANES. Previously reported XPS analyses[11] showed that Pd was present predominantly in the metallic state, with a small fraction in PdO form, and no noticeable changes in Pd speciation were observed between the catalysts prepared under oxic and reducing solution conditions.

EXAFS Analysis of the Oxidized Catalyst. Figure 4 shows the Re L_{III} edge EXAFS data obtained for the 5 wt % Re catalyst exposed to oxic solution conditions. The $k^3\chi(k)$ plot (Figure 4A) is similar to the solid and dissolved forms of the NH_4ReO_4 reference standard. However, the catalyst spectrum more closely matches that of dissolved NH_4ReO_4 and has slightly larger amplitude than solid NH_4ReO_4. It is unlikely that the amplitude differences occurred because of sample thickness effects, as the measured transmission edge step for all three samples was $\Delta\mu x$ = 0.9−1.2. In addition, the postedge features in the XANES spectra of solid NH_4ReO_4 (arrow in Figure S2) should also be suppressed if thickness effects were causing the decreased white line intensity. Instead, the reduction in amplitude in the EXAFS of the solid NH_4ReO_4 reference standard is likely due to increased disorder in the ReO_4 tetrahedron when it crystallizes. The magnitude of the Fourier Transform (FT; Figure 4B) consists of a single peak centered at $R + \Delta$ = 1.4 Å. The data were fit using only the single scattering Re−O path derived from the crystal structure of NH_4ReO_4, and the best-fit structural parameters are listed in Table 1. The coordination number of 4.2 ± 0.3 is consistent with the

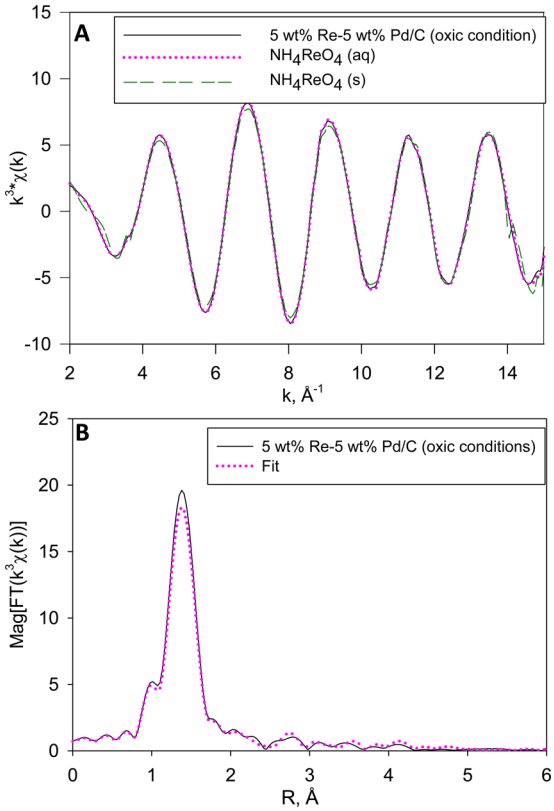

Figure 4. (A) Comparison of Re L_{III} edge EXAFS $k^3\chi(k)$ spectrum of 5 wt % Re−5 wt % Pd/C collected from water under oxic conditions (continuous air sparging) with Re^{VII} reference standards, and (B) magnitude of Fourier transform (FT) of $k^3\chi(k)$ data for the catalyst and fit using Re−O path.

Table 1. Best Fit Parameters of Re L_{III} Edge EXAFS Spectra of Catalysts

path description	CN[a]	R^b (Å)	$\Delta E^{0,c}$	σ^{2d} ($\times 10^{-3}$ Å^2)	x^e
5 wt % Re−5 wt % Pd/C Collected from Water under Oxic Conditions					
Re−O	4.2 ± 0.3	1.74 ± 0.01	1.6 ± 1.7	1 ± 0.3	
12 wt % Re−5 wt % Pd/C Collected from Water under Reducing Conditions					
Re−O	6.3 ± 0.6	2.03 ± 0.01	5.2 ± 1.3	5 ± 0.7	
Re−Re	3.0 ± 0.6	2.57 ± 0.01	5.2 ± 1.3	4 ± 0.7	
0.5 wt % Re−5 wt % Pd/C under H_2-Reducing Condition					
Re−O and Re−Re paths with fixed parameters (shown above) from the fits of 12 wt % Re−5 wt % Pd/C catalyst					0.28
Re−O	1.3 ± 1.3	2.45 ± 0.03	0.5 ± 3.8	3 ± 7	0.72
Re−Pd	3.4 ± 2.4	2.72 ± 0.03	6.4 ± 5.5	8 ± 4	

[a]CN: average number of neighboring atoms in a shell. [b]R: average distance between the absorbing atom and the neighboring atoms. [c]ΔE^0: energy shift. [d]σ^2: relative mean-square displacement of the atom pairs of the path. [e]x: a fractional fitting parameter.

tetrahedral structure of ReO_4^-, and the Re−O interatomic distance of 1.74 ± 0.01 Å is identical to the distance previously reported for ReO_4^- (i.e., 1.73 Å).[32] The similarity between the EXAFS data for the catalyst sample under oxic conditions and that for dissolved NH_4ReO_4 supports the conclusion that Re is present as hydrated ReO_4^- ions that associate with the Pd/C catalyst surface via outer-sphere complexation mechanisms (e.g., electrostatic, H-bonding).

EXAFS Analysis of the Reduced Catalysts. Figure 5 shows $k^3\chi(k)$ EXAFS data obtained for Re−Pd/C samples

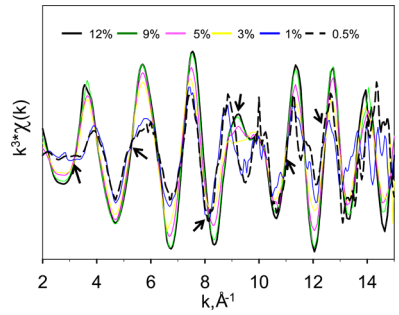

Figure 5. Re L_{III} edge EXAFS $k^3\chi(k)$ spectra of 0.5 wt % to 12 wt % Re−5 wt % Pd/C collected from water under reducing conditions. Arrows highlight a few isosbestic points.

exposed to reducing solution conditions with Re content ranging from 0.5 to 12 wt %. Consistent changes in the spectra are observed as Re content is increased, with multiple isosbestic points in the spectral overlays (e.g., at 3.1, 4.2, 5.3, 7.3 Å^{-1}). The trends suggest the presence of two major Re species on the catalyst surface, the proportions of which change gradually with Re content. The spectra obtained for catalysts with 9 and 12 wt % Re are identical within the experimental uncertainty. This suggests that no further changes in the average coordination environment occur beyond 9 wt % Re loading and that a single Re species dominates at the upper end of the bimetallic compositional range examined. In contrast, spectra obtained for the two catalyst samples at the lower end of the compositional range (0.5 and 1 wt % Re) differ from one another, indicating that both of the major Re species contribute to measured spectra at these conditions.

EXAFS spectra of the two compositional endmembers (i.e., 12 and 0.5 wt % Re) were quantitatively analyzed to identify the local atomic structure of the two major contributing Re species immobilized on the surface of reduced Re−Pd/C catalysts. First, for the catalyst with 12 wt % Re, the magnitude of the FT[$k^3\chi(k)$] (Figure 6A) shows two dominant peaks in the $R + \Delta$ region between 1 and 3 Å. No significant peaks are present at $R + \Delta > 3$ Å, indicating a lack of long-range crystalline order in the immobilized Re species. FT data in the region $R + \Delta = 1.2$−3.0 Å were fit best using single scattering Re−O and Re−Re paths. Attempts to fit the spectrum using a Re−Pd path in place of Re−Re resulted in a significantly inferior fit of the measured second shell FT features (not shown). The best-fit structural parameters are summarized in Table 1. The coordination number for the Re−O path is 6.3 ± 0.6 and the coordination number for the Re−Re path is 3.0 ± 0.6, with interatomic distances of 2.03 ± 0.01 and 2.57 ± 0.01 Å, respectively. The measured spectrum is reproduced well by this model, as illustrated by the contributions of each path to the real part of FT[$k^3\chi(k)$]. The Re−O bond distance is in the range reported for Re^{IV} and Re^{V} standards (i.e., 1.87−2.29 Å)[31] and longer than that seen in Re^{VII} standards (i.e., 1.73 Å).[32] The Re−Re interatomic distance is shorter than that in Re metal or ReO_2 (i.e., 2.75 and 2.62 Å, respectively).[31,35] The presence of Re−O and Re−Re backscattering and the lack of longer range structure in the FT suggests that Re is present in the form of oxorhenium clusters on the surface of the carbon support material. The refined Re−O and Re−Re coordination numbers and distances suggest a cluster in which ReO_6

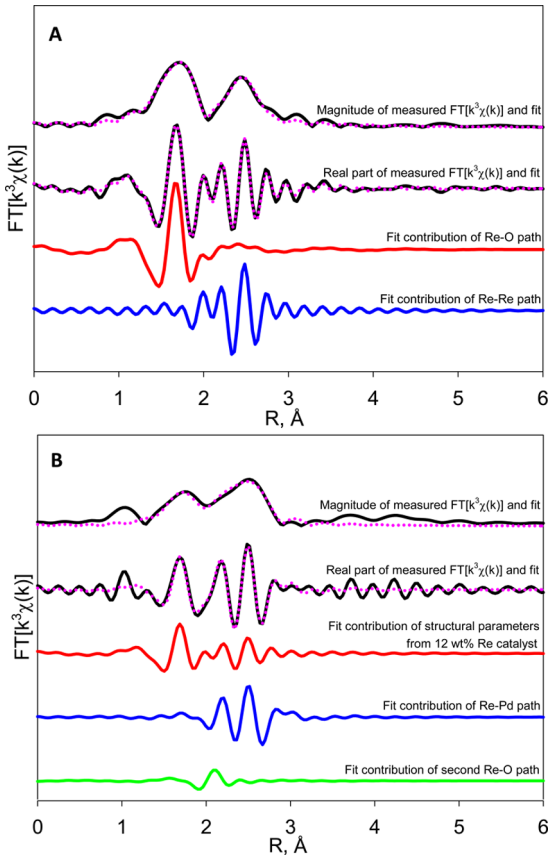

Figure 6. FT of measured $k^3\chi(k)$ data for (A) 12 wt % Re−5 wt % Pd/C catalyst and fit using Re−O and Re−Re paths and (B) 0.5 wt % Re−5 wt % Pd/C catalyst and its fit using Re−O, Re−Re, and Re−Pd paths. For magnitude and real part of FT$[k^3\chi(k)]$, solid lines indicate measured data and dotted lines indicate fits. Catalysts were collected from water under reducing conditions.

octahedra are coordinated to each other in an edge sharing configuration, either planar or pyramidal (Figure 7A). Similar "raft" and cluster structures for Re on the surface of γ-Al_2O_3 supports have been previously proposed based on EXAFS characterization.[18,36]

Figure 6B shows the measured FT$[k^3\chi(k)]$ and fit for the other compositional endmember (0.5 wt % Re catalyst). As discussed above, these data are significantly different from the next member in the series (i.e., 1 wt % Re catalyst). Thus, it is assumed that both of the major reduced Re species contribute to the observed spectrum of the 0.5 wt % sample. To obtain structural parameters for the second reduced Re endmember (the one assumed to become significant at lower Re loading), the fits of the spectrum of the 0.5 wt % sample included the spectrum for the Re species that predominates in the 12 wt % Re catalyst weighted by a fractional content variable. This was achieved by fixing the parameters for the Re−O and Re−Re paths to the values refined in the fits of the 12 wt % Re endmember and multiplying the coordination numbers by a fractional fitting parameter x ($0 < x < 1$). This approach is equivalent to adding the 12 wt % Re catalyst data as a component in a linear combination fit. The other component contributing to the measured spectrum was then fit using combinations of unconstrained Re−O, Re−Re, and Re−Pd single scattering paths. The best fit of the 0.5 wt % Re sample (Figure 6B) was obtained by combining 28% of the Re species that predominates at 12 wt % Re with 72% of a second species described by Re−O and Re−Pd single-scattering paths (i.e., x = 0.28). The best-fit structural parameters for the second species (Table 1) have an average coordination of 1.3 O (or possibly C) atom at 2.45 ± 0.03 Å and 3.4 Pd atoms at 2.72 ± 0.03 Å. Attempts to fit the data with a Re coordination shell (instead of Pd) resulted in a lower quality fit, with the reduced χ^2 goodness-of-fit parameter being 2.4 times larger than that obtained using a Pd shell. The lack of Re−Re backscattering contributions in the second immobilized Re species suggests that the majority of the Re is present as monomeric species adsorbed to the Pd sites. The edge position and the large amplitude of the XANES white line for the sample suggests that Re is more oxidized than metallic Re. The fit-derived Re−Pd distance of 2.72 ± 0.03 Å is similar to the 2.67 Å distance observed for metallic Re−Pd clusters by Meitzner et al.[20] The lack of appropriate Re standards (e.g., Re−Pd alloys or ionic Re of low valence) makes it difficult to propose a structural model, but the results show that Re is coordinated to Pd sites as a low valence monomeric Re species (formal valence of 1 or 2).

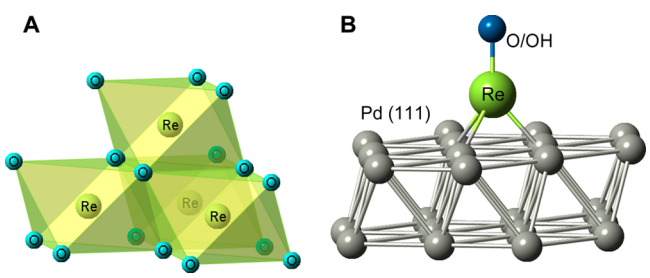

Figure 7. Proposed structures of Re species immobilized on Re−Pd/C consistent with EXAFS fitting results. (A) Oxorhenium(V) cluster species that predominates on catalysts with higher Re content. The pyramidal cluster of four edge-sharing Re octahedra results in an average Re−Re coordination number of 3. (B) Monomeric hydroxorhenium(I) species directly coordinated to three Pd sites on the surface of Pd nanoclusters.

Distribution of Reduced Re Species in Catalysts with Varying Re Content. To quantify the relative contribution of the two identified Re species in the catalyst samples with increasing Re content, the $k^3\chi(k)$ data were fit using linear combinations of the two endmember spectra calculated by using the structural parameters listed in Table 1. Plots of the two Re species (hereafter referred to as "Re monomeric" and "Re cluster" species) and an example fit of the measured spectra for catalyst samples with 5 wt % are shown in Figure 8A. Figure 8B summarizes the results of the linear combination fits of all the catalyst samples, illustrating the gradual shift in predominance from the Re monomeric species at lower Re wt % to the Re cluster species at higher Re wt %. The general trend is qualitatively similar to that observed with XPS results (Figure 3C). However, the distribution of species derived from XPS indicates somewhat greater contribution of the more reduced Re monomeric species at all catalyst compositions examined, suggesting that this species may be enriched at the outer surface of the micrometer-sized porous catalyst support particles relative to the bulk material probed by XAS. That said, the differences between XAS and XPS are small and may also be an artifact resulting from sample drying required for the latter technique.

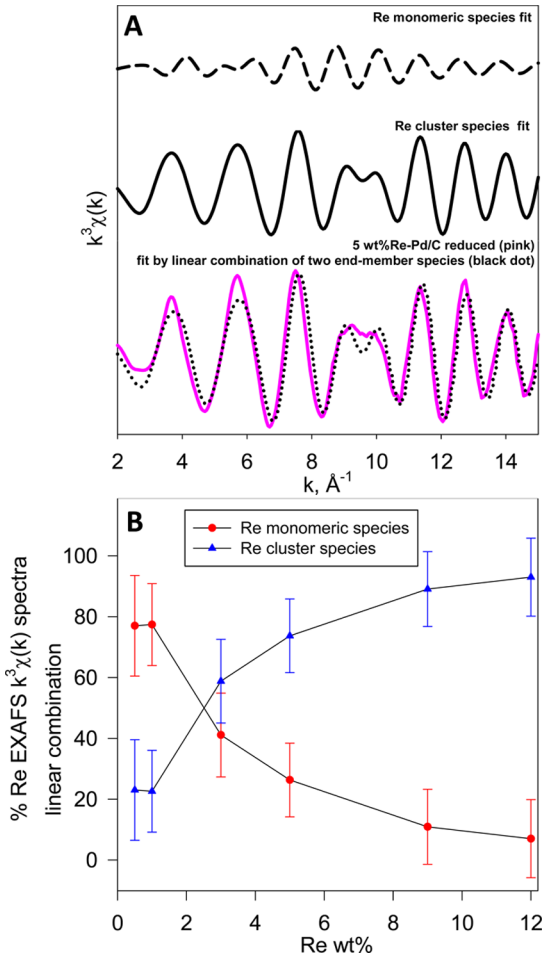

Figure 8. (A) Re L_{III} edge EXAFS $k^3\chi(k)$ spectra of 5 wt % Re−5 wt % Pd/C catalyst collected from water under reducing conditions and fit using linear combination of two Re species derived from fitting (Re monomeric species and Re cluster species), and (B) proportions of two Re species contributions obtained by linear combination fits for catalysts with varying Re content. Error bars indicate 95% confidence levels.

■ DISCUSSION

Re−Pd/C Catalysts under Oxic Solution Conditions. Characterization of Re speciation in oxidized Re−Pd/C catalysts is relevant to Re dynamics in the following cases: (1) when the catalyst is exposed to water containing sufficient concentration of dissolved oxygen for Re to be oxidized, and (2) when Re is oxidized in the oxygen-atom transfer (OAT) reaction with ClO_4^- ions faster than it is being re-reduced (e.g., when treating elevated concentrations of oxyanions). XAS and XPS analyses of oxidized catalyst samples indicate similarity to the NH_4ReO_4 reference standards, particularly the dissolved form, suggesting that immobilized Re is oxidized to Re^{VII}. The lack of EXAFS spectral contributions from a second coordination shell indicates that mononuclear ReO_4^- ions are adsorbed to the carbon support (or possibly Pd nanocluster sites on the support) by outer-sphere long-range electrostatic and/or hydrogen bonding mechanisms. This association of Re^{VII} to the surface under aqueous conditions is different from that reported for dry alumina-supported Re catalysts prepared at high temperature (>500 °C), where inner-sphere Re−O−Al linkages were observed.[16,17] The outer-sphere adsorption mechanism has implications for the in operando stability of Re catalysts used for water treatment since ReO_4^- ions adsorbed by outer-sphere interactions are likely to be more prone to leaching due to ion exchange with other anionic constituents present in the solution matrix being treated. Thus, close examination of Re leaching during catalytic treatment, especially for proposed treatment applications in high salinity environments like waste ion exchange brines,[10] is warranted.

Re−Pd/C Catalysts under Reducing Solution Conditions (Active State for ClO_4^- Reduction). XANES spectra of catalysts with Re loading >5 wt % that are exposed to reducing solution conditions are similar to those of the Re^{IV} and Re^{V} reference standards, and application of an empirical correlation (Figure 2B) yields an average Re valence throughout the catalyst material of +4.8 when the Re content reaches 12 wt %. Applying this same correlation shows that the average valence becomes more reduced at lower Re content, reaching a value of +1.6 for 0.5 wt % Re. A similar trend is observed using surface-sensitive XPS, with spectra of individual catalyst samples being fit by combinations of spectral features most consistent with Re^{I} and Re^{V} reference standards; the contribution to spectral fits shifts in favor of the former at lower Re content and the latter at higher Re content.

Evidence for shifting Re speciation with Re loading is also present in the EXAFS data. Fitting of the data from the 12 wt % Re catalyst suggests that Re is present predominantly in the form of oxorhenium clusters consisting of about 4−6 Re atoms each (Figure 7A). The first- and second-shell interatomic distances are consistent with the Re coordination in both ReO_2 and Re_2O_5.[37] However, the XPS spectrum of the 12 wt % Re catalyst shows a Re $4f_{7/2}$ peak with BE that is 1.0 eV higher than that of ReO_2, suggesting a Re species that is more oxidized than Re^{IV}. Furthermore, OAT reactions converting the metal between Re^{VII} and Re^{V} and between Re^{V} and Re^{III} have been reported,[38,39] whereas, to the best of our knowledge, there are no reports of OAT reactions involving Re^{IV} species like ReO_2. Tests also showed no reaction between aqueous ClO_4^- and ReO_2 powder within 24 h (sufficient time for complete reduction of ClO_4^- with Re−Pd/C). Thus, we conclude that the predominant Re species present under reducing conditions in the high Re content catalysts is an oxorhenium(V) cluster species. The Re−Re coordination number determined from the EXAFS analysis suggests that these are clusters 5−12 Å in diameter.[40] The small size is consistent with STEM-EDS imaging of the 12 wt % Re−5 wt % Pd/C catalyst, which shows no obvious Re phases in association with or away from the observed metallic Pd nanoclusters (data not shown). Although the proposed structural model is well supported by the EXAFS data, future theoretical studies (e.g., density functional theory) may provide insight on its compatibility with observed stability or reactivity data. The agglomeration of several Re atoms effectively reduces exposed surface area and would additionally contribute to decreased redox reactivity with oxidants relative to isolated, more reduced Re ions.

The more reduced Re species that predominates at lower Re loadings exhibits characteristics of monomeric species. The binding energy measured by XPS for this species is 1.2 eV higher than that of metallic Re (BE = 40.1 eV), and the $k^3\chi(k)$ EXAFS spectra of the 0.5 wt % Re catalyst does not match well with Re metal. Ducros et al.[41] reported a BE of 41.2 eV for Re metal exposed to oxygen. They estimated that approximately 2 Å thickness of oxide layer was formed on top of Re and hypothesized that oxidized Re species are in the form of Re_2O (+1 oxidation sate) or ReO (+2 oxidation state). Tysoe et al.[21]

found that while the Re species in a Pt–Re alloy were found to be Re metal (BE = 39.7 eV), thermal H_2 treatment of a Re film deposited on Pt foil yielded a fraction of Re with BE = 40.8 eV. The latter is 1.1 eV higher than that of Re metal and was interpreted as an oxorhenium phase formed on the surface of Pt. Fits of the EXAFS data of Re–Pd/C catalyst with 0.5 wt % Re loading also show a first shell containing 1 oxygen atom, supporting the conclusion of an oxorhenium species rather than metallic Re. The EXAFS data support direct coordination of this Re species with the Pd nanoclusters deposited on the activated carbon support material. It is possible that adsorption to specific Pd sites stabilizes a highly reduced monomeric oxorhenium Re species (Figure 7B). A tetrahedral structure of low-valence Re complex (i.e., +1 oxidation state) with one hydroxide ligand has been previously reported.[42]

The fits of the XPS spectra and the linear combination analysis of the EXAFS data indicate that the monomeric Pd-coordinated Re^I species predominate at low Re wt % and that the proportion of the oxidic Re^V clusters increases with increased Re loading. Both EXAFS (Figure 8B) and XPS (Figure 3C) data show this same general trend, but the exact distributions of Re species determined from the two methods quantitatively differ. The differences may be explained by the different nature of two spectroscopic characterization methods. XPS is a surface-sensitive vacuum technique that identifies chemical states of Re at the surface (1–10 nm);[33] XAS, on the other hand, is a bulk analysis technique that characterizes the average Re speciation throughout the Re–Pd/C material. The activated carbon catalyst support is a porous material where exterior surfaces most likely have higher accessibility to both Re precursor (i.e., ReO_4^-) and hydrogen than interior pores. Therefore, the difference in the proportion of Re species between EXAFS and XPS results suggests that Re^I species are more likely to be formed at exterior particle surfaces where interactions of Pd, Re precursor, and hydrogen are possibly enriched relative to the materials present deeper within the porous material structure. Drying samples for XPS may also produce enhanced Re interaction with the surface and lead to shifts in Re oxidation state.

Based on spectroscopic results, a Re catalyst reduction process can be proposed wherein the ReO_4^- precursor is immobilized on the Pd/C catalyst suspended in H_2-saturated aqueous solution ($[H_2]_{aq} \approx 0.8$ mM when $P_{H_2} = 1$ bar), and the initial fraction of Re is reductively immobilized preferentially near the surface of the Pd^0 nanoclusters. Since H_2 dissociates to atomic hydrogen at Pd, it is reasonable to assume that the ReO_4^- ions nearest to the Pd sites will have greater opportunity for reaction with Pd-adsorbed atomic hydrogen (Pd–H_{ads}) and be reduced to ReOH via the following reaction,

$$Re^{VII}O^-_{4(ads)} + 6Pd{-}H_{ads} + H^+ \rightarrow Re^IOH_{(ads,Pd)} + 6Pd + 3H_2O \quad (1)$$

As Re loading increases, available Pd sites for direct Re–Pd binding become saturated. However, due to atomic hydrogen spillover,[43] ReO_4^- associated with the carbon support surface can still be reduced to oxorhenium(V) clusters:

$$2ReO^-_{4(ads)} + 4H_{(spillover)} + 2H^+_{(aq)} \rightarrow Re^V_2O_{5(ads,C)} + 3H_2O \quad (2)$$

Potential reasons for the lower extent of Re reduction may include that "spillover" atomic H is not as strong of reductant as Pd-adsorbed atomic H or that Re bonded to Pd is more readily reduced. Theoretical studies may be able to provide more insight into these interactions.

Influence of Re Speciation on Catalytic Activity. Previous work demonstrated ClO_4^- reduction using Re–Pd/C formulations with Re loading ranging from 1 to 12 wt %.[9] This suggests that both the Re^I monomeric and Re^V cluster species can react with ClO_4^-. Therefore, the proposed catalytic OAT mechanism for ClO_4^- reduction (Figure 1) is modified to include reactions for Re^I in addition to Re^V. In principle, redox cycling between odd valence oxorhenium species can be accomplished by OAT reactions:

$$Re^{VII}O_4^- \overset{OAT}{\Longleftrightarrow} Re^{VII}O_3^- \overset{OAT}{\Longleftrightarrow} Re^{VII}O_2^- \overset{OAT}{\Longleftrightarrow} Re^IO^- \quad (3)$$

OAT reactions from Re^V to Re^{VII} and Re^{III} to Re^V have been reported previously.[10,29,30] Thus, it may be hypothesized that Re^I species can also participate in OAT reactions and abstract oxygen from kinetically inert ClO_4^- and other oxyanion daughter products (Figure 9). Our previous study showed

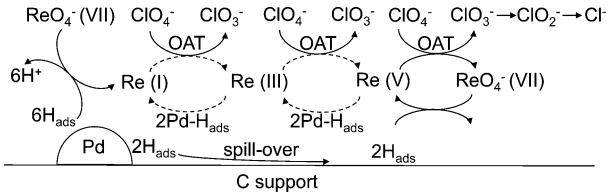

Figure 9. Modified oxygen atom transfer (OAT) reactions scheme for ClO_4^- reduction on Re–Pd/C catalysts involving Pd-adsorbed atomic hydrogen and atomic hydrogen that spills over to sites on the carbon support material. Dashed arrow indicates possible sequential OAT reactions from Re^I species to Re^V species.

that mass-normalized reactivity of Re with respect to perchlorate reduction was higher at low Re content (Figure S6 in SI). This may indicate that Re^I monomeric species are more reactive with ClO_4^- than Re^V cluster species. A higher catalytic reactivity of Re^I species would suggest that (1) the OAT reaction between ClO_4^- and $Re^IOH_{(ads,Pd)}$ is faster than the reaction between ClO_4^- and $Re^V_2O_{5(ads,C)}$ and (2) rereduction of Re from higher oxidation state to Re^I monomeric species is faster than to Re^V cluster species during the catalytic cycle due to the close proximity of Re^I species to the Pd surface where H_2 dissociates. Alternatively, it is possible that the monomeric Re^I species that predominate at low loading are more accessible (i.e., have a higher surface area per unit Re immobilized) than the Re^V cluster species that predominate at higher Re loading.

■ CONCLUSIONS

In summary, XAS and XPS were used to characterize the speciation of Re immobilized on Re–Pd/C catalysts that have shown promise for treating water contaminated with perchlorate, a highly recalcitrant and toxic oxyanion that has been widely detected in drinking water resources. Under oxic solution conditions (i.e., water equilibrated with the atmosphere), Re associates with the Pd/C catalyst surface by attraction of mononuclear ReO_4^- ions via outer-sphere electrostatic and/or hydrogen bonding interactions. When solutions are exposed to H_2, atomic hydrogen formed by H_2 dissociation on Pd/C reduces the ReO_4^- ions to two strongly adsorbed species. For catalysts with low Re content (e.g., ≤ 1

wt %), monomeric oxorhenium(I) species that are directly coordinated to Pd nanoclusters (e.g., ReOH) predominate, whereas oxorhenium(V) clusters (e.g., Re_4O_{10}) predominate at higher Re loading (e.g., 5−12 wt %). Based on the these findings, we propose that adsorbed ReO_4^- precursors closest to the Pd nanoclusters are first reduced to Re^I species by Pd−H_{ads}, and additional Re more distant from the Pd nanoclusters are reduced to Re^V species by atomic hydrogen spillover onto the activated carbon support surface. A revised catalytic OAT reaction scheme is proposed invoking redox cycling between odd-valence Re species (+1, +3, +5, +7) and reaction of ClO_4^- and daughter oxyanion species with Re^I and Re^V.

■ ASSOCIATED CONTENT

Supporting Information

Overlays of XANES spectra of Re−Pd/C catalysts exposed to oxic and reducing solution conditions and EXAFS analysis of ReO_2 and NH_4ReO_4 reference standards. This material is available free of charge via the Internet at http://pubs.acs.org.

■ AUTHOR INFORMATION

Corresponding Author

*Phone: (217) 244-4679. E-mail: strthmnn@illinois.edu.

Notes

The authors declare no competing financial interest.

■ ACKNOWLEDGMENTS

This work was supported by NSF Chemical, Bioengineering, Environmental, and Transport Systems (CBET-0730050 and CBET-0746453) and U.S. EPA (RD-83517401). We thank John Shapley (UIUC) and Danmeng Shuai (George Washington Univ.) for insightful discussion and technical feedback. We also thank the staff of MR-CAT for assistance with beamline setup. MR-CAT is supported by the U.S. Department of Energy under Contract DE-FG01-94-ER45525 and the member institutions. Use of the Advanced Photon Source was supported by the U.S. Department of Energy under Contract W-31-109-Eng-38. Rick Haasch is acknowledged for assistance with XPS, which was carried out in the Frederick Seitz Material Research Laboratory Central Facilities, University of Illinois.

■ REFERENCES

(1) Crabtree, R. H. *The Organometallic Chemistry of the Transition Metals*; John Wiley & Sons: New York, 2011.

(2) Mol, J. C. Olefin Metathesis over Supported Rhenium Oxide Catalysts. *Catal. Today* **1999**, *51*, 289−299.

(3) Schwarz, D. E.; Frenkel, A. I.; Nuzzo, R. G.; Rauchfuss, T. B.; Vairavamurthy, A. Electrosynthesis of ReS_4. XAS Analysis of ReS_2, Re_2S_7, and ReS_4. *Chem. Mater.* **2004**, *16*, 151−158.

(4) Lagos, G.; García, R.; Agudo, A. L.; Yates, M.; Fierro, J. L. G.; Gil-Llambías, F. J.; Escalona, N. Characterisation and Reactivity of Re/carbon Catalysts in Hydrodesulphurization of Dibenzothiophene: Effect of Textural and Chemical Properties of Support. *Appl. Catal., A-Gen.* **2009**, *358*, 26−31.

(5) Hilbrig, F.; Michel, C.; Haller, G. L. A XANES-TPR Study of Platinum-Rhenium/Alumina Catalysts. *J. Phys. Chem.* **1992**, *96*, 9893−9899.

(6) Kunkes, E. L.; Simonetti, D. A.; Dumesic, J. A.; Pyrz, W. D.; Murillo, L. E.; Chen, J. G.; Buttrey, D. J. The Role of Rhenium in the Conversion of Glycerol to Synthesis Gas over Carbon Supported Platinum−Rhenium Catalysts. *J. Catal.* **2008**, *260*, 164−177.

(7) Lobo-Lapidus, R. J.; Gates, B. C. Rhenium Complexes and Clusters Supported on γ-Al_2O_3: Effects of Rhenium Oxidation State and Rhenium Cluster Size on catalytic Activity for *n*-Butane Hydrogenolysis. *J. Catal.* **2009**, *268*, 89−99.

(8) Vardon, D. R.; Sharma, B. K.; Jaramillo, H.; Kim, D.; Choe, J. K.; Ciesielski, P. N.; Strathmann, T. J. Hydrothermal Catalytic Processing of Saturated and Unsaturated Fatty Acids to Hydrocarbons with Glycerol for in situ Hydrogen Production. *Green Chem.* **2014**, *16*, 1507−1520.

(9) Hurley, K. D.; Shapley, J. R. Efficient Heterogeneous Catalytic Reduction of Perchlorate in Water. *Environ. Sci. Technol.* **2007**, *41*, 2044−2049.

(10) Liu, J.; Choe, J. K.; Sasnow, Z.; Werth, C. J.; Strathmann, T. J. Application of a Re−Pd Bimetallic Catalyst for Treatment of Perchlorate in Waste Ion-Exchange Regenerant Brine. *Water Res.* **2013**, *47*, 91−101.

(11) Choe, J. K.; Shapley, J. R.; Strathmann, T. J.; Werth, C. J. Influence of Rhenium Speciation on the Stability and Activity of Re/Pd Bimetal Catalysts used for Perchlorate Reduction. *Environ. Sci. Technol.* **2010**, *44*, 4716−4721.

(12) Abu-Omar, M. M.; Appelman, E. H.; Espenson, J. H. Oxygen-Transfer Reactions of Methylrhenium Oxides. *Inorg. Chem.* **1996**, *35*, 7751−7757.

(13) Urbansky, E. T. American Chemical Society: Division of Environmental Chemistry. *Perchlorate in the Environment*; Springer: New York, 2000.

(14) Wang, D. M.; Shah, S. I.; Chen, J. G.; Huang, C. P. Catalytic Reduction of Perchlorate by H_2 Gas in Dilute Aqueous Solutions. *Sep. Purif. Technol.* **2008**, *60*, 14−21.

(15) Bunker, G. *Introduction to XAFS: A Practical Guide to X-ray Absorption Fine Structure Spectroscopy*; Cambridge University Press: Cambridge, U.K.; New York, 2010.

(16) Hardcastle, F. D.; Wachs, I. E.; Horsley, J. A.; Via, G. H. The Structure of Surface Rhenium Oxide on Alumina from Laser Raman Spectroscopy and X-ray Absorption Near-Edge Spectroscopy. *J. Mol. Catal.* **1988**, *46*, 15−36.

(17) Bare, S. R.; Kelly, S. D.; D.Vila, F.; Boldingh, E.; Karapetrova, E.; Kas, J.; Mickelson, G. E.; Modica, F. S.; Yang, N.; Rehr, J. J. Experimental (XAS, STEM, TPR, and XPS) and Theoretical (DFT) Characterization of Supported Rhenium Catalysts. *J. Phys. Chem. C* **2011**, *115*, 5740−5755.

(18) Fung, A. S.; Kelley, M. J.; Koningsberger, D. C.; Gates, B. C. γ-Al_2O_3-Supported Re−Pt Cluster Catalyst Prepared from [$Re_2Pt(CO)_{12}$]: Characterization by Extended X-ray Absorption Fine Structure Spectroscopy and Catalysis of Methylcyclohexane Dehydrogenation. *J. Am. Chem. Soc.* **1997**, *119*, 5877−5887.

(19) Daniel, O. M.; DeLaRiva, A.; Kunkes, E. L.; Datye, A. K.; Dumesic, J. A.; Davis, R. J. X-ray Absorption Spectroscopy of Bimetallic Pt−Re Catalysts for Hydrogenolysis of Glycerol to Propanediols. *ChemCatChem.* **2010**, *2*, 1107−1114.

(20) Meitzner, G.; Via, G. H.; Lytle, F. W.; Sinfelt, J. H. Structure of Bimetallic Clusters. Extended X-ray Absorption Fine Structure (EXAFS) of Pt−Re and Pd−Re Clusters. *J. Chem. Phys.* **1987**, *87*, 6354−6363.

(21) Tysoe, W. T.; Zaera, F.; Somorjai, G. A.; An, X. P. S. Study of the Oxidation and Reduction of the Rhenium-Platinum System under Atmospheric Conditions. *Surf. Sci.* **1988**, *200*, 1−14.

(22) Parshall, G. W.; Shive, L. W.; Cotton, F. A. Phosphine Complexes of Rhenium. In *Inorganic Syntheses*; MacDiarmid, A. G., Ed.; John Wiley & Sons, Inc.: New York, 2007; pp 110−112.

(23) Arnáiz, F. J.; Pedrosa, M. R.; Aguado, R.; McPherson, L. D.; Béreau, V. M.; Abu-Omar, M. M.; Salzer, A.; Bauer, A.; Geyser, S.; Podewils, F.; et al. Organometallic and Coordination Complexes. In *Inorganic Syntheses*; Shapley, J. R., Ed.; John Wiley & Sons, Inc.: New York, 2004; pp 49−95.

(24) Franco, D.; Gómez, M.; Jiménez, F.; Muller, G.; Rocamora, M.; Maestro, M. A.; Mahía, J. Exo- and Endocyclic Oxazolinyl−Phosphane Palladium Complexes: Catalytic Behavior in Allylic Alkylation Processes. *Organometallics* **2004**, *23*, 3197−3209.

(25) Hurley, K. D. Heterogeneous Catalytic Reduction of Perchlorate in Water, University of Illinois at Urbana Champaign: Illinois, 2008.

(26) Kropf, A.; Katsoudas, J.; Chattopadhyay, S.; Shibata, T.; Lang, E.; Zyryanov, V. N.; Ravel, B.; Mclvor, K.; Kemner, K. M.; Scheckel, K. G. The new MRCAT (Sector 10) Bending Magnet Beamline at the Advanced Photon Source. *SRI 2009: The 10th International Conference On Synchrotron Radiation Instrumentation* **2010**, *1234*, 299−302.
(27) Ravel, B. ATOMS: Crystallography for the X-ray Absorption Spectroscopist. *J. Synchrotron Radiat.* **2001**, *8*, 314−316.
(28) Ravel, B.; Newville, M. ATHENA, ARTEMIS, HEPHAESTUS: Data Analysis for X-ray Absorption Spectroscopy Using ıt IFEFFIT. *J. Synchrotron Radiat.* **2005**, *12*, 537−541.
(29) Newville, M. IFEFFIT: Interactive XAFS Analysis and FEFF Fitting. *J. Synchrotron Radiat.* **2001**, *8*, 322−324.
(30) Ankudinov, A. L.; Ravel, B.; Rehr, J. J.; Conradson, S. D. Real-Space Multiple-Scattering Calculation and Interpretation of X-ray-Absorption Near-Edge Structure. *Phys. Rev. B* **1998**, *58*, 7565−7576.
(31) Corrêa, H. P. S.; Cavalcante, I. P.; Martinez, L. G.; Orlando, C. G. P.; Orlando, M. T. D. Refinement of Monoclinic ReO_2 Structure from XRD by Rietveld Method. *Braz. J. Phys.* **2004**, *34*, 1208−1210.
(32) Kruger, G. J.; Reynhardt, E. C. Ammonium Perrhenate at 295 and 135 K. *Acta Crystallogr., Sect. B* **1978**, *34*, 259−261.
(33) Van der Heide, P. *X-ray Photoelectron Spectroscopy: An Introduction to Principles and Practices*; John Wiley & Sons, Inc.: Hoboken, NJ, 2012.
(34) Conradson, S. D. XAFS—A Technique to Probe Local Structure. *Los Alamos Sci.* **2000**, *26*, 422−435.
(35) Pauling, L. Atomic Radii and Interatomic Distances in Metals. *J. Am. Chem. Soc.* **1947**, *69*, 542−553.
(36) Fung, A.; Tooley, P.; Kelley, M.; Koningsberger, D.; Gates, B. Cationic Trirhenium Rafts on Gamma-Alumina: Characterization by X-ray Absorption Spectroscopy. *J. Phys. Chem.* **1991**, *95*, 225−234.
(37) Borisova, L. V.; Ryabchikov, D. I.; Yarinova, T. I. Rhenium Compounds in Sulfuric Acid Solutions in the Presence of Reducing Agents. *Russ. J. Org. Chem.* **1968**, *13*, 321−328.
(38) Abu-Omar, M. M.; Espenson, J. H. Facile Abstraction of Successive Oxygen Atoms from Perchlorate Ions by Methylrhenium Dioxide. *Inorg. Chem.* **1995**, *34*, 6239−6240.
(39) Conry, R. R.; Mayer, J. M. Oxygen Atom Transfer Reactions of Cationic Rhenium (III), Rhenium (V), and Rhenium (VII) Triazacyclononane Complexes. *Inorg. Chem.* **1990**, *29*, 4862−4867.
(40) Jentys, A. Estimation of Mean Size and Shape of Small Metal Particles by EXAFS. *Phys. Chem. Chem. Phys.* **1999**, *1*, 4059−4063.
(41) Ducros, R.; Alnot, M.; Ehrhardt, J. J.; Housley, M.; Piquard, G.; Cassuto, A. A Study of the Adsorption of Several Oxygen-Containing Molecules (O_2, CO, NO, H_2O) on Re(0001) by XPS, UPS and Temperature Programmed Desorption. *Surf. Sci.* **1980**, *94*, 154−168.
(42) Tahmassebi, S. K.; Conry, R. R.; Mayer, J. M. Low-Valent Rhenium-oxo Compounds. 12. Rearrangement of a Rhenium Hydroxide Complex to an oxo-hydride Compound. *J. Am. Chem. Soc.* **1993**, *115*, 7553−7554.
(43) Contescu, C. I.; Brown, C. M.; Liu, Y.; Bhat, V. V.; Gallego, N. C. Detection of Hydrogen Spillover in Palladium-Modified Activated Carbon Fibers during Hydrogen Adsorption. *J. Phys. Chem. C* **2009**, *113*, 5886−5890.